Inorg. Chem. **2005**, *44*, 3137–3145

The Gas Phase Structure of Ethynylferrocene Using Microwave Spectroscopy

Ranga Subramanian, Chandana Karunatilaka, Kristen S. Keck, and Stephen G. Kukolich*

Department of Chemistry, University of Arizona, Tucson, Arizona 85721

Received October 21, 2004

Gas phase structural parameters for ethynylferrocene have been determined using microwave spectroscopy. Rotational transitions due to *a*- and *b*-type dipole moments were measured. Twenty four rotational constants have been determined by fitting the measured transitions of various isotopomers using a rigid rotor Hamiltonian with centrifugal distortion constants. Least-squares fits to determine structural parameters and Kraitchman analyses have been used to determine the gas phase structural parameters and the atomic coordinates from the rotational constants. The distance between the Fe atom and the C atoms of the cyclopentadienyl rings is $r(\mathrm{Fe–C_1}) = 2.049(5)$ Å, and the distance between the carbon atoms of the cyclopentadienyl ring is $r(\mathrm{C–C}) = 1.432(2)$ Å. The ethynyl group is bent away from the Fe atom and out of the plane of the carbon atoms in the adjacent cyclopentadienyl ring by 2.75(6)°. Structural parameters were also obtained from DFT calculations and Kraitchman analyses, and the results are compared. Analysis of fit results for ^{13}C isotopic substitution data indicates that the carbon atoms of the two cyclopentadienyl rings are in an eclipsed conformation in the ground vibrational state. Trends in microwave experimental values for the distance from the Fe atom to the center of the cyclopentadienyl ring for a series of substituted ferrocenes have been analyzed. This analysis provides an estimate of the gas phase distance from the Fe atom to the centers of the cyclopentadienyl rings for ferrocene of 1.65(1) Å.

Introduction

There are many useful correlations between structure and reactivity for organometallic compounds. Microwave spectroscopy can be used to accurately determine the effects of substituents on the molecular structures of ferrocenes and other complexes. In the present work, the basic structural parameters are determined for ethynylferrocene and compared with similar parameters for other substituted ferrocenes.

Ethynylferrocene (ETHFE) is an attractive synthon used to synthesize many polymeric ferrocenyl organometallic compounds.[1,2] These poly-ynes, in general, find applications as organic conductors,[3] in optoelectronic applications and photonics,[4,5] as part of a quantum-dot cellular automaton,[6] and as metalloethynyl nanoparticles with thermo set properties.[7] Given the importance of this compound, ETHFE has been studied using ^{57}Fe NMR,[8] ^{13}C NMR,[9] Mössbauer spectroscopy,[10] and electrochemical studies in solution.[11] These methods provide a better understanding of the electronic properties of this compound. Previous studies on the various substituted ferrocene compounds have shown that there are linear correlations between some of the experimentally measured electronic properties. The electronic properties that were correlated are oxidation potentials from electrochemical studies in solution, ^{57}Fe quadrupole splittings obtained using Mössbauer spectroscopy in the solid phase, and gas phase ionization energies from photoelectron spectroscopy.[11−14] The proposed reason for the above linear correlations is that the main contribution to the highest

* Author to whom correspondence should be addressed. E-mail: kukolich@u.arizona.edu.

(1) Sato, M.; Hayashi, Y.; Shintate, H.; Katada, M.; Kawata, S. *J. Organomet. Chem.* **1994**, *471*, 179−184.
(2) Ingham, S. L.; Khan, M. S.; Lewis, J.; Long, N. J.; Raithby, P. *J. Organomet. Chem.* **1994**, *470*, 153−159.
(3) Zyss, J.; Chemla, D. S. *NonLinear Optical Properties of Organic Molecules and Crystals*; Academic Press: New York, 1987; Vol. I
(4) Meyers, F.; Marder, S. R.; Pierce, B. M.; Bredas, J. L. *J. Am. Chem. Soc.* **1994**, *116*, 10703−10714.
(5) Hide, F.; Diaz-Garcia, M. A.; Schqartz, B. J.; Heeger, A. *Acc. Chem. Res.* **1997**, *30*, 430−436.
(6) Li, Z.; Beatty, A. M.; Fehlner, P. T. *Inorg. Chem.* **2003**, *42*, 5707−5714.
(7) Keller, T. M.; Perrin, J.; Qadri, S. U.S. Patent Application Publ., 2003.
(8) Haslinger, E.; Robien, W.; Schlögl, K.; Weissensteiner, W. *J. Organomet. Chem.* **1981**, *218*, C11−C17.
(9) Koridze, A. A.; Petrovskii, P. V.; Mokhov, A. I.; Lutsenko, A. I. *J. Organomet. Chem.* **1977**, *136*, 57−63.
(10) Schottenberger, H.; Buchmeiser, M. R.; Herber, R. H. *J. Organomet. Chem.* **2000**, *612*, 1−8.
(11) Strelets, V. V. *Russ. Chem. Rev.* **1989**, *58*, 297−311.

10.1021/ic048516x CCC: $30.25
Published on Web 03/29/2005

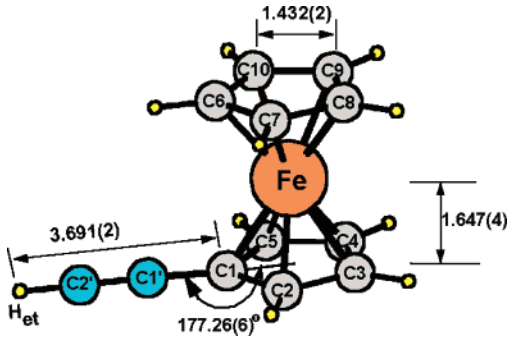

Figure 1. Structure of ETHFE with the different atoms of the molecule labeled. The values of the four parameters that were varied are indicated along with the uncertainties. The units of the distances are Å, and the units of the angle are degrees. The ethynyl group is tilted by 2.7(1)° out of the Cp plane, in a direction away from the Fe atom.

occupied molecular orbital (HOMO) and the lowest unoccupied molecular orbital (LUMO) for these complexes is the atomic orbital of the metals.[15] However, we believe that it is also important to have accurate and precise structural data, so that there will be a better understanding of structural, chemical, and electronic properties. Previously, the structure of this complex was determined using X-ray diffraction,[16,17] which indicated the existence of a weak hydrogen bond between the ethynyl hydrogen of one ETHFE molecule and the π triple bond of the −CCH group of another ETHFE molecule. These weak hydrogen bonds along with other crystal packing effects present in the solid phase distort the "true structure" of the molecule. Because these effects are absent in the gas phase, the structural determination of this molecule using Fourier transform gas phase microwave spectroscopy was undertaken. In previous work,[18−21] we have been successful in determining the structure of various substituted ferrocene compounds.

In the present work, the microwave spectra of ETHFE and 1-deuterio-2-ferrocenylethyne (DETHFE) have been recorded. The spectra of the ETHFE ^{56}Fe, ^{54}Fe, ^{57}Fe, and ^{13}C isotopomers and the DETHFE ^{56}Fe isotopomer have been recorded in the frequency range of 4−12 GHz. Rotational constants were determined by a least-squares fitting of the assigned transitions. From these rotational constants, structural parameters of the molecule were obtained using a structural least-squares analysis and from Kraitchman analyses. Comparisons of the theoretical and X-ray data with the gas phase microwave data provide a more complete understanding of the structure of ETHFE. Furthermore, by combining results from the previous microwave studies on substituted ferrocenes with the present work, the correlations of a gas phase structural parameter, namely the distance between the iron atom and the cyclopentadienyl (Cp) ring, with the Hammett parameter ($\Sigma\sigma_I$) and with the redox potential of the molecule have been analyzed. Figure 1 shows the structure of ETHFE with all of the carbon atoms labeled.

Experiment

The ETHFE was purchased from Aldrich (catalog number: 44265−8) and used as received. The preparation of DETHFE was based on the modified synthesis of ferrocenylpropyne.[22,23] In a drybox, a round-bottom flask was prepared containing 1.0 g of ETHFE, 30 mL of anhydrous ether, and a stir bar. The dark red crystals dissolved readily, giving a deep orange solution. In addition, 8.0 mL of 1.6 M *n*-butyllithium (Li^{n}Bu) in hexane and 10 mL of anhydrous ether were placed in a separate round-bottom flask. Outside the drybox, the orange-yellow-tinged Li^{n}Bu solution was syringed into the ETHFE solution at −78 °C, causing the solution to become darker. The solution was warmed to room temperature and stirred overnight. Then, 1.5 mL of D_2O was syringed into the solution at 0 °C. The reaction was instantaneous, causing the solution to lighten and give a glutinous white precipitate. The liquid was transferred to a smaller flask via syringe, and the solvent was removed at room temperature and 20 Torr, with the residual solvent removed at 0.5 Torr. Upon bringing the flask back to atmospheric pressure with the addition of nitrogen, the resultant liquid solidified. The solid was then sublimed at 0.5 Torr and 40 °C using a cold-water finger for collection. The dark red air-stable crystals were used without further purification. This synthesis leads to deuterium substitution at the ethynyl hydrogen site, H_{et} (see Figure 1).

The pulsed-jet Fourier transform microwave spectrometer used for the current experiment is explained elsewhere in detail.[24] This type of spectrometer system was originally developed by Flygare and Balle[25] and has "opened the door" to microwave measurements on a wide variety of organometallic compounds. Both compounds were heated above the melting point to 60 °C to obtain sufficient vapor pressure, and the pressure of the neon carrier gas was maintained at 0.5 atm. This mixture was pulsed into the Fabry Perot cavity at a constant pulse rate of 2 Hz. A low-noise liquid-nitrogen-cooled amplifier increased the sensitivity and improved the signal-to-noise ratio significantly, which facilitated obtaining the transitions of different isotopomers in natural abundance. Thirty nine transitions were recorded for the ^{56}Fe isotopomer, and 11 transitions were observed for ^{54}Fe (6% natural abundance), while five transitions each were observed for ^{57}Fe (2% natural abundance) and the four ^{13}C isotopomers (2% natural abundance). In the case of DETHFE, 20 transitions were recorded for ^{56}Fe. An example of a portion of the spectrum is given in Figure 2 to illustrate a typical observed molecular transition.

Theoretical Methods

Different theoretical methods and basis sets were used to find the best structure for ETHFE. The two methods used were DFT,

(12) Roberts, R. M. G.; Silver, J. *J. Organomet. Chem.* **1984**, *263*, 235−241.
(13) Al-Saeed, A. M.; Seddon, E. A.; Seddon, K. R.; Shimran, A. A.; Tompkins, S.; Grossel, M. C.; Knychala, J. P. *J. Organomet. Chem.* **1988**, *347*, C25−C30.
(14) Matsumura-Inoue, T.; Kuroda, K.; Umezawa, Y.; Achiba, Y. *J. Chem. Soc., Faraday Trans. 2* **1989**, *85*, 857−866.
(15) Green, J. C. *Struct. Bonding (Berlin)* **1981**, *43*, 37−112.
(16) Wurst, K.; Elsner, O.; Schottenberger, H. *Synlett* **1995**, *8*, 833−834.
(17) Steiner, T.; Tamm, M.; Grzegorzewski, A.; Schulte, N.; Veldman, N.; Schreurs, A. M. M.; Kanters, J. A.; Kroon, J.; van der Maas, J.; Lutz, B. *J. Chem. Soc., Perkin Trans.* **1996**, *11*, 2441−2446.
(18) Drouin, B. J.; Lavaty, T. G.; Cassak, P. A.; Kukolich, S. G. *J. Chem. Phys.* **1997**, *107*, 6541−6548.
(19) Drouin, B. J.; Dannemiller, J. J.; Kukolich, S. G. *J. Chem. Phys.* **2000**, *112*, 747−751.
(20) Margolis, D. S.; Tanjaroon, C.; Kukolich, S. G. *J. Chem. Phys.* **2002**, *117*, 3741−3747.
(21) Tanjaroon, C.; Keck, K. S.; Kukolich, S. G. *J. Am. Chem. Soc.* **2004**, *126*, 844−850.
(22) Abram, T. S.; Crawford, W.; Knipe, A. C.; Watts, W. E. *Proc. R. Ir. Acad., Sect. B* **1977**, *77B*, 317−321.
(23) Doisneau, G.; Balavoine, G.; Fillebeen-Khan, T. *J. Organomet. Chem.* **1992**, *425*, 113−117.
(24) Bumgarner, R. E.; Kukolich, S. G. *J. Chem. Phys.* **1987**, *86*, 1083−1089.
(25) Balle, T. J.; Flygare, W. H. *Rev. Sci. Instrum.* **1981**, *52*, 33.

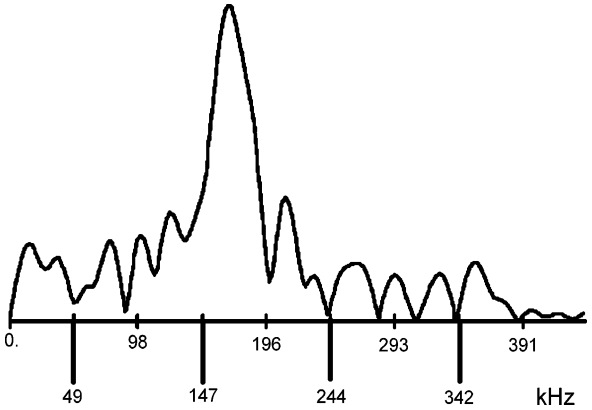

Figure 2. Fourier transform spectrum of the $4_{13} \leftarrow 3_{12}$ transition for the molecule ETHFE. The *x* axis shows the offset frequency in kHz from the stimulating frequency of 6 141 730 kHz. This spectrum is an average of five shots.

using Becke's three-parameter functional with the nonlocal correlation provided by Perdew and Wang (B3PW91)[26−28] and MP2 (Møller−Plesset correlation energy correction truncated at second-order[29−32]). The basis sets used are (1) the Los Alamos double-ζ basis set (LANL2DZ),[33−35] (2) the Dunning/Huzinaga valence double-ζ on carbon and hydrogen atoms with Stuggart/Dredsen electron core potentials on the iron atoms (SDD),[35,36] (3) Stuggart potentials on all atoms except for the hydrogen atoms (SDDAll),[35] and (4) the Hay and Wadt (n+1) basis set with an effective core potential for iron[39] and a split-valence plus polarization basis set (SVP)[40,41] for the carbon and hydrogen atoms.

All geometry optimization methods were followed with frequency analysis to ensure that the stationary points found were at least local minima. The B3PW91 calculations with different basis sets predict structural parameters and rotational constants closer to the experimental values. In the case of the MP2 method, the calculations with different basis sets predict smaller structural parameters and higher rotational constants compared to those from the microwave experiment. This is consistent with the fact that the MP2 method tends to underestimate bond lengths.[37,38] The success of the B3PW91 calculation to produce near experimental quality results is consistent with the usage of the "best" exchange-correlation potentials for these molecules.[37] An energy optimization starting from the staggered conformation of the molecule using any of the above methods and basis sets resulted in rotation to the eclipsed conformer. This indicates that the eclipsed conformer is the lower energy conformation.

The preferred method and basis set used to predict the geometry and structure of ETHFE is B3PW91 and the Hay and Wadt (n+1) basis set with an effective core potential for iron[39] and the split-valence plus polarization basis set (SVP)[40,41] for the carbon and hydrogen atoms. This combination was preferred because it allowed us to predict the rotational constants closer to the experimental values and resulted in a shorter initial search for the rotational transitions of the molecule ETHFE.

All of the theoretical calculations were done on an HP/Compaq Alpha supercomputer (AURA) using Gaussian 03 programs[42] at the University of Arizona.

Data Analysis

The observed transitions for the various isotopomers are listed in Tables 1−4. These transitions were fit using a least-squares-fitting program, SPFIT,[43] which employs a standard rigid rotor Hamiltonian with centrifugal distortion constants. Following this fitting procedure, a program, piform,[44] was used to correct the unusual uncertainties from the SPFIT program and, thereby, obtain the values of the various constants with more conventional standard errors. For ETHFE with the normal isotopes ($^{12}C_{12}$, $^{1}H_{10}$, and ^{56}Fe), transitions were fit using five adjustable parameters, the three rotational constants (*A*, *B*, and *C*) along with two distortion constants (Δ_j and Δ_k). In the case of the other observed isotopomers of the molecule (^{54}Fe, ^{57}Fe, $^{13}C_{2,5}$, $^{13}C_{3,4}$, $^{13}C_{9,8}$, and $^{13}C_{7,10}$), the observed transitions were fit using the rotational constants as adjustable parameters while holding the distortion constants Δ_j and Δ_k fixed to the values obtained from the normal isotopomer fit. For the synthesized compound, DETHFE, the transitions were fit using four adjustable parameters, the three rotational constants (*A*, *B*, and *C*) along with a distortion constant (Δ_j). The values obtained for these parameters are given in Table 5.

For an accurate determination of the rotational constants for different low-abundance isotopomers, four transitions were measured and fit. A prediction resulting from this least-squares fit was used to find and measure the fifth transition, which was then added to the least-squares fit. This procedure

(26) Becke, A. D. *J. Chem. Phys.* **1993**, *98*, 5648−5652.
(27) Perdew, J. P.; Wang, Y. *Phys. Rev. B: Condens. Matter* **1992**, *45*, 13244−13249.
(28) Lee, C.; Yang, W.; Parr, R. G. *Phys. Rev. B: Condens. Matter* **1987**, *37*, 785−789.
(29) Head-Gordon, M.; Pople, J. A.; Frisch, M. J. *Chem. Phys. Lett.* **1988**, *153*, 503−506.
(30) Frisch, M. J.; Head-Gordon, M.; Pople, J. A. *Chem. Phys. Lett.* **1990**, *166*, 275−280.
(31) Frisch, M. J.; Head-Gordon, M.; Pople, J. A. *Chem. Phys. Lett.* **1990**, *166*, 281−289.
(32) Head-Gordon, M.; Head-Gordon, T. *Chem. Phys. Lett.* **1994**, *220*, 122−128.
(33) Hay, P. J.; Wadt, W. R. *J. Chem. Phys.* **1985**, *82*, 270−283.
(34) Wadt, W. R.; Hay, P. J. *J. Chem. Phys.* **1985**, *82*, 284−298.
(35) Dunning, T. H., Jr.; Hay, P. J. In *Modern Theoretical Chemistry*; Schaefer, H. F., III, Ed.; Plenum: New York, 1976; Vol. 3.
(36) Cao, X. Y.; Dolg, M. *THEOCHEM* **2002**, *581*, 139−147.
(37) Swart, M.; Snijders, J. G. *Theor. Chem. Acc.* **2003**, *110*, 34−41.
(38) Klopper, W.; Lüthi, H. P. *Chem. Phys. Lett.* **1996**, *262*, 546−552.
(39) Hay, P. J.; Wadt, W. R. *J. Chem. Phys.* **1985**, *82*, 299−310.
(40) Schaefer, A.; Horn, H.; Ahlrichs, R. *J. Chem. Phys.* **1992**, *97*, 2571−2577.
(41) Schaefer, A.; Huber, C.; Ahlrichs, R. *J. Chem. Phys.* **1994**, *100*, 5829−5835.
(42) Frisch, M. J.; Trucks, G. W.; Schlegel, H. B.; Scuseria, G. E.; Robb, M. A.; Cheeseman, J. R.; Montgomery, J. A., Jr.; Vreven, T.; Kudin, K. N.; Burant, J. C.; Millam, J. M.; Iyengar, S. S.; Tomasi, J.; Barone, V.; Mennucci, B.; Cossi, M.; Scalmani, G.; Rega, N.; Petersson, G. A.; Nakatsuji, H.; Hada, M.; Ehara, M.; Toyota, K.; Fukuda, R.; Hasegawa, J.; Ishida, M.; Nakajima, T.; Honda, Y.; Kitao, O.; Nakai, H.; Klene, M.; Li, X.; Knox, J. E.; Hratchian, H. P.; Cross, J. B.; Adamo, C.; Jaramillo, J.; Gomperts, R.; Stratmann, R. E.; Yazyev, O.; Austin, A. J.; Cammi, R.; Pomelli, C.; Ochterski, J. W.; Ayala, P. Y.; Morokuma, K.; Voth, G. A.; Salvador, P.; Dannenberg, J. J.; Zakrzewski, V. G.; Dapprich, S.; Daniels, A. D.; Strain, M. C.; Farkas, O.; Malick, D. K.; Rabuck, A. D.; Raghavachari, K.; Foresman, J. B.; Ortiz, J. V.; Cui, Q.; Baboul, A. G.; Clifford, S.; Cioslowski, J.; Stefanov, B. B.; Liu, G.; Liashenko, A.; Piskorz, P.; Komaromi, I.; Martin, R. L.; Fox, D. J.; Keith, T.; Al-Laham, M. A.; Peng, C. Y.; Nanayakkara, A.; Challacombe, M.; Gill, P. M. W.; Johnson, B.; Chen, W.; Wong, M. W.; Gonzalez, C.; Pople, J. A. *Gaussian 03*, rev. B.05; Gaussian, Inc.: Pittsburgh, PA, 2003.
(43) Pickett, H. M. *J. Mol. Spectrosc.* **1991**, *148*, 371−377.
(44) This program is authored by Dr. Zbigniew Kisiel and can be obtained along with the instructions for use from the website http://info.ifpan-.edu.pl/~kisiel/prospe.htm.

Table 1. Observed Transitions for ETHFE (^{56}Fe) with Fit Residuals[a]

J	K_a	K_c	J'	K_a'	K_c'	observed frequencies	O − C[b] (in kHz)
4	1	4	3	1	3	5508.9887(7)	0
4	0	4	3	0	3	5612.4794(5)	−1
4	2	3	3	2	2	5870.0694(6)	3
4	1	3	3	1	2	6141.5547(8)	−5
4	2	2	3	2	1	6154.9149(5)	1
5	0	5	4	1	4	6789.6572(5)	6
5	1	5	4	1	4	6846.0279(9)	−4
3	2	1	2	0	2	6906.5691(3)	−6
5	0	5	4	0	4	6907.7906(7)	−1
5	1	5	4	0	4	6964.1625(6)	−9
4	2	3	3	1	2	7109.9023(9)	13
5	2	4	4	2	3	7294.0854(9)	1
5	4	2	4	4	1	7450.6159(10)	10
5	3	3	4	3	2	7451.8403(2)	14
5	4	1	4	4	0	7454.9440(7)	11
5	3	2	4	3	1	7543.8060(6)	−3
5	1	4	4	1	3	7580.0008(0)	−4
5	2	3	4	2	2	7754.3000(7)	−10
6	0	6	5	1	5	8145.8013(7)	3
6	1	6	5	1	5	8170.7894(7)	−6
6	0	6	5	0	5	8202.1719(7)	−7
6	1	6	5	0	5	8227.1695(6)	−6
6	1	5	5	1	4	8947.4157(7)	−6
6	4	3	5	4	2	8961.3337(4)	5
6	4	2	5	4	1	8980.0638(8)	−12
7	0	7	6	1	6	9477.2806(6)	−2
7	1	7	6	1	6	9487.8382(6)	7
7	0	7	6	0	6	9502.2773(5)	−2
7	1	7	6	0	6	9512.8255(5)	−3
7	2	6	6	2	5	10065.5264(6)	8
7	1	6	6	1	5	10254.1113(10)	−1
7	3	5	6	3	4	10403.6780(7)	6
8	0	8	7	1	7	10796.3438(6)	12
8	1	8	7	1	7	10800.6283(11)	−3
8	0	8	7	0	7	10806.8797(7)	−1
8	1	8	7	0	7	10811.1813(6)	1
7	2	5	6	2	4	10825.9805(7)	3
8	1	7	7	1	6	11533.3875(6)	0
8	3	6	7	3	5	11844.8633(11)	−11

[a] The observed frequencies are given in MHz. The numbers within the parentheses are the errors in the observed values. [b] Observed − calculated.

Table 2. Observed Transitions for ETHFE (^{54}Fe) with Fit Residuals[a]

J	K_a	K_c	J'	K_a'	K_c'	observed frequencies	O − C[b] (in KHz)
4	0	4	3	0	3	5614.9548(3)	−5
4	1	3	3	1	2	6144.3761(4)	0
5	1	5	4	1	4	6849.1628(3)	7
5	0	5	4	0	4	6910.8490(8)	−5
5	1	4	4	1	3	7583.3794(6)	−8
6	1	6	5	1	5	8174.5117(9)	−2
6	0	6	5	0	5	8205.8486(6)	0
6	2	5	5	2	4	8696.5267(6)	4
6	1	5	5	1	4	8951.3047(7)	3
7	1	7	6	1	6	9492.1436(6)	−1
7	1	6	6	1	5	10258.4922(8)	2

[a] The observed frequencies are given in MHz. [b] Observed − calculated.

helped to verify that the initial assignments were correct. Even though the molecule has two dipole moment components, *a* and *b*, the transitions due to the *b* dipole are at least four times weaker. Hence, only the strong *a*-type dipole transitions were observed for the low-abundance isotopomers.

Structure Determination

Least-Squares Fit. The least-squares structural fits were done by adjusting the structural parameters to obtain the best fit to the 24 rotational constants from the various isotopomers. For the least-squares fit, a coordinate system is defined such that the *z*-axis origin is at the Fe atom and passes through the center of the two Cp rings. The *x* axis is perpendicular to the *z* axis, passes through the Fe atom, and lies parallel to the ethynyl group. The *y* axis is perpendicular to the *x* and *z* axes. This definition of the cylindrical coordinate system automatically defines the Fe atom to be at the origin, with the *x* and *z* axes defining the symmetry plane of the molecule. The plane defined by the *x* and *z* axes is also the *a*−*b* plane of the molecule. Thus, during the least-squares fit, the molecule is constrained to belong to C_s point group symmetry. This is experimentally proven by the observation of only one set of unique rotational constants for each pair of ^{13}C atoms related by reflection in the *a*−*b* plane ($^{13}C_{2,5}$, $^{13}C_{3,4}$, $^{13}C_{9,8}$, $^{13}C_{7,10}$). It is further assumed that the two Cp rings have C_5 symmetry. This assumption that deviations from C_5 symmetry for the Cp rings are small enough to be neglected is supported by the DFT calculations and the results of the Kraitchman analyses. For chloroferrocene,[19] many more isotopomers were measured in order to determine these distortions, but values were barely larger than uncertainties.

Different structural fits were done to decide which structural parameters could be unambiguously determined. From the analysis of the correlation effects, a particular set of four structural parameters was found to be the best determinable set. These four parameters are (1) the distance from the Fe to the center of the Cp ring, r(Fe−Cp), (2) the carbon−carbon bond length of the Cp ring, r(C−C), (3) the angle that the ethynyl group (−C≡CH) makes with the Cp ring, also called the "tilt angle", a(Cp−CCH), and (4) the C_1−H_{et} length of the ethynyl functional group, $r(C_1-H_{et})$. The "best fit" values obtained are (1) r(Fe−Cp) = 2.048 68(5) Å, (2) r(C−C) = 1.43152(2) Å, (3) "tilt angle" a(Cp−CCH) = 2.75(6)°, and (4) $r(C_1-H_{et})$ = 3.692(2) Å. The above listed uncertainties, for the first three parameters, only include the statistical uncertainty from the least-squares fit. When the effects of correlation of the variable parameters, with parameters not directly determined in the fit, are included, the uncertainties become much larger. These values, and more reliable uncertainties, are shown in Figure 1, which also shows the structure of the complex. The distances from the Fe atoms to the center of the two Cp rings were assumed to be the same. For a test fit where the distances were independently varied, the resulting values for the two r(Fe−Cp) distances came out the same, within the uncertainties. The initial starting structure for the least-squares fit was based on the results from the DFT calculations. Because deuterium substitutions were not made on the Cp ring, the C−H bond distances of the Cp ring were all fixed at 1.088 Å and the radial symmetry of the C−H bonds was maintained during the fit. These C−H bond lengths are quite unlikely to be in error by more than 0.002 Å, and so we do not believe that this constraint introduces further error. There was no attempt made to vary the $C_5H_4C_2H$ moiety tilt angle with respect to the C_5H_5Fe moiety; this angle was maintained at 0°.

The structural fit obtained as described above yielded a standard deviation of 0.02 MHz. This is considered an excellent fit because the rotational constants are over 1000

Table 3. Observed Transitions of ETHFE Isotopomers ^{57}Fe, $^{13}C_{2,5}$, $^{13}C_{3,4}$, $^{13}C_{9,8}$, and $^{13}C_{7,10}$ with Fit Residuals[a]

transitions		^{57}Fe		$^{13}C_{2,5}$		$^{13}C_{3,4}$		$^{13}C_{9,8}$		$^{13}C_{7,10}$	
$J'_{Ka'Kc'}$	J_{KaKc}	observed	O − C	observed	O − C	observed	O − C	observed	O − C	observed	O − C
4_{14}	3_{13}	5507.7363(5)	−2	5492.0286(6)	0	5484.1597(5)	−1			5483.8733(6)	0
4_{04}	3_{03}	5611.2563(8)	3	5594.6730(6)	2	5583.9710(5)	1	5574.8493(5)	−1	5586.3698(4)	2
4_{13}	3_{12}	6140.1636(5)	3	6118.5098(6)	0	6124.7100(4)	2	6091.7310(7)	−1	6110.5531(6)	0
5_{15}	4_{14}	6844.4877(5)	0					6798.2861(6)	1		
5_{05}	4_{04}			6886.5474(2)	−2	6871.5008(5)	1	6862.1738(5)	−1	6876.1657(3)	−2
5_{14}	4_{13}	7578.3216(11)	−3	7552.2662(6)	−1	7552.7558(9)	−2	7522.5024(6)	1	7542.1230(6)	−1

[a] The observed frequencies are given in MHz, and observed − calculated (O − C) values are given in kHz. The numbers within the parentheses are the errors in the observed values.

Table 4. Observed Transitions for DETHFE (^{56}Fe) with Fit Residuals[a]

J	K_a	K_c	J'	K_a'	K_c'	observed frequencies	O − C[b] (in KHz)
3	1	2	2	1	1	4524.1716(6)	9
4	1	4	3	1	3	5357.1468(5)	−1
4	0	4	3	0	3	5460.9570(4)	1
4	2	3	3	2	2	5712.3099(4)	3
4	1	3	3	1	2	5980.5916(6)	3
4	2	2	3	2	1	5990.1286(7)	5
5	1	5	4	1	4	6657.1315(5)	−7
5	0	5	4	0	4	6719.7188(6)	−3
5	2	4	4	2	3	7098.1478(4)	2
5	1	4	4	1	3	7381.9297(5)	−1
6	1	6	5	1	5	7944.9679(2)	−5
6	0	6	5	0	5	7977.0929(4)	0
6	1	5	5	1	4	8714.0073(3)	−3
7	1	7	6	1	6	9225.0881(8)	3
7	0	7	6	0	6	9240.0148(6)	3
7	2	6	6	2	5	9795.0508(4)	−6
7	1	6	6	1	5	9985.7122(7)	3
7	3	5	6	3	4	10125.5462(10)	−11
8	0	8	7	0	7	10507.4404(9)	6
8	1	7	7	1	6	11228.9206(6)	1

[a] The observed frequencies are given in MHz. The numbers within the parentheses are the errors in the observed values. [b] Observed − calculated.

MHz. The Cartesian coordinates (in Å) obtained in the principal axis system from the least-squares fit are given in the Table 6, and all of the parameters derived from this structure are given in Table 7. The estimated uncertainties are 0.02 Å for these coordinates, because most were not fit directly. These values are based on fixing the bond distances $r(C_1-C_{1'})$ and $r(C_{1'}-C_{2'})$ (see Table 7) at the values of 1.4214 and 1.2173 Å, respectively. These fixed bond lengths were obtained from the B3PW91 calculations outlined in the Theoretical Methods section of this paper earlier. We believe that the value of $r(C_1-H_{et})$ is quite accurately determined from the fit. However, because the bond distances $r(C_1-C_{1'})$ and $r(C_{1'}-C_{2'})$ and $r(C_{2'}-H_{et})$ are correlated, the uncertainty in the value of $r(C_{2'}-H_{et})$ will depend on the accuracy of the calculated values for $r(C_1-C_{1'})$ and $r(C_{1'}-C_{2'})$. The value of a(Cp−CCH) indicates that the ethynyl group deviates out of the plane of the Cp ring, in a direction away from the Fe atom by 2.75(6)°, and C_1 and C_6 are eclipsed (see Figure 1).

Kraitchman Analysis. As we have not measured all of the ^{13}C and deuterium-substituted isotopomers, a complete substitution structure was not obtained. Nonetheless, the present substitution structural coordinates obtained are close to the least-squares fit values and provide support for the accuracy of the least-squares fit parameters and the assumption that the basic C_5 symmetry is maintained. The various structural parameters derived from the Kraitchman analysis are given in Table 7.

Given the fact that the Kraitchman analysis uses the changes in the moments of inertia due to the monosubstitution of different atoms in the molecule and that the moments of inertia are related to the square of the coordinates of the substituted atoms, one can obtain only the absolute values of these coordinates. These absolute values of the coordinates determined in the principal axis system of the parent molecule are given in Table 8. There was no ambiguity in assigning the absolute values of these coordinates to the correct atoms nor in the signs of the coordinates obtained. The best indication that the gas phase structure of ETHFE is "eclipsed" is obtained from the least-squares fit results, which do not converge for the staggered conformation, and the theoretical calculations, which favor the eclipsed conformation.

We believe that the nonzero coordinates obtained along the c principal axis for the substituted atoms ^{54}Fe, ^{57}Fe, H_{et}, and $^2H_{et}$ represent root-mean-square values due to the vibrational averaging present in the molecule, and these values were set to zero when the internal parameters were calculated using the Kraitchman coordinates (Table 7). The Fe parameters derived from the Kraitchman analysis (see Table 7) are obtained by using ^{54}Fe a_s, b_s, and c_s coordinates, because this isotopomer has more assigned transitions, and therefore, better determined coordinates are obtained when compared to the ^{57}Fe substitution results.

Correlation of Structural Changes with the Hammett Parameters. A comparison between the parameters obtained for different substituted ferrocene compounds is shown in Table 9. These values are obtained from previous microwave studies[18−21] for all of the compounds except ferrocene. The values of the parameters for ferrocene (X = H and Y = H) are obtained from the electron diffraction structure.[45]

As one can observe from Table 9, the r(C−C) bond length does not change among the different complexes but the r(Fe−Cp) distance changes significantly. This trend can be related to the electronegativity of the substitution on Cp; that is, an increase in electronegativity decreases the r(Fe-Cp) distance. We therefore observe a linear correlation between the gas phase structural parameter r(Fe-Cp) and the inductive Hammett parameter[12] $\Sigma\sigma_I$, which is proportional to the electronegativity of the substituent group (see Table 9). A linear regression analysis was done between the parameters

(45) Haaland, A.; Nilsson, J. E. *Acta Chem. Scand.* **1968**, *22*, 2653−2670.

Table 5. Spectral Parameters Obtained for the Different Isotopomers of ETHFE (^{56}Fe, ^{54}Fe, ^{57}Fe, $^{13}C_{2,5}$, $^{13}C_{3,4}$, $^{13}C_{9,8}$, and $^{13}C_{7,10}$) and DETHFE (^{56}FeD), Determined Using Least-Squares Fits[a]

parameter	^{56}Fe	^{54}Fe	^{57}Fe	$^{13}C_{2,5}$
A	1307.397 (4)	1307.611(6)	1307.286(1)	1299.909(8)
B	819.8373(3)	820.2258(8)	819.644(1)	816.4342(4)
C	654.6347(4)	654.9374(2)	654.4854(4)	652.8387(3)
Δ_j	0.000031(3)	[0.000031(3)][b]	[0.000031(3)][b]	[0.000031(3)][b]
Δ_k	0.0051(6)	[0.0051(6)][b]	[0.0051(6)][b]	[0.0051(6)][b]
σ(fit)	0.007	0.004	0.002	0.001
number of lines	39	11	5	5

parameter	$^{13}C_{3,4}$	$^{13}C_{9,8}$	$^{13}C_{7,10}$	^{56}FeD
A	1292.414(8)	1305.623(7)	1298.380(9)	1286.793(5)
B	819.0830(5)	812.2979(4)	815.4798(5)	798.7219(4)
C	651.2160(3)	650.2266(2)	651.8125(4)	636.1039(4)
Δ_j	[0.000031(3)][b]	[0.000031(3)][b]	[0.000031(3)][b]	0.000042(4)
Δ_k	[0.0051(6)][b]	[0.0051(6)][b]	[0.0051(6)][b]	
σ(fit)	0.005	0.001	0.004	0.005
number of lines	5	5	5	20

[a] All of the values listed are in units of MHz, and the error limits are 1σ. [b] Held fixed during the fit.

Table 6. Coordinates (in Å) for ETHFE Obtained from a Least-Squares Fit, Given in the Principal Axis System

atom	*a*	*b*	*c*
Fe	−0.385	−0.178	0.000
C_6	−0.868	1.813	0.000
C_7	−1.408	1.167	1.158
C_8	−2.281	0.122	0.716
C_9	−2.281	0.122	−0.716
C_{10}	−1.408	1.167	−1.158
H_6	−0.178	2.639	0.000
H_7	−1.194	1.422	2.182
H_8	−2.839	−0.546	1.349
H_9	−2.839	−0.546	−1.349
H_{10}	−1.194	1.422	−2.182
C_1	1.660	−0.301	0.000
C_2	1.120	−0.946	1.158
C_3	0.247	−1.991	0.716
C_4	0.247	−1.991	−0.716
C_5	1.120	−0.946	−1.158
H_1	1.334	−0.691	2.182
H_2	−0.311	−2.659	1.349
H_3	−0.311	−2.659	−1.349
H_4	1.334	−0.691	−2.182
$C_{1'}$	2.519	0.833	0.000
$C_{2'}$	3.307	1.761	0.000
H_{et}	3.990	2.565	0.000

for the five substituted molecules. This analysis results in an equation (eq 1) with the regression statistics $r = 0.93$. The least-squares regression line obtained is shown in Figure 3.

$$r(\text{Fe}-\text{Cp}) = -0.0821\Sigma\sigma_I + 1.6585 \qquad (1)$$

Furthermore, a linear correlation is observed between the gas phase structural distance r(Fe−Cp) and the ferrocene/ferrocenium redox potential at ambient temperatures relative to the ferrocene (Fc) standard.[46,47] Thus, the ΔE^0 values are given by the equation, E^{ox}(Fc−X) − E^{ox}(Fc−H), where E^{ox}(Fc−X) is the oxidation potential of the ferrocenyl derivatives and E^{ox}(Fc−H) is the oxidation potential of the ferrocene. A linear regression analysis was done, and the plot is shown in Figure 4. The following equation (eq 2) was obtained from this analysis and the value of $r = 0.91$.

$$r(\text{Fe}-\text{Cp}) = -0.1499\Delta E^0 + 1.6509 \qquad (2)$$

The error bars on the data points along the *y* axis in both Figures 3 and 4 reflect the uncertainties present in the microwave gas phase values for the r(Fe−Cp) parameter. Extrapolating the gas phase data for r(Fe−Cp) for the substituted ferrocenes, in this manner, allows us to obtain an approximate gas phase value for unsubstituted ferrocene of r(Fe−Cp) = 1.65(1) Å.

Table 7. Structural Parameters Obtained for the ETHFE Molecule[a]

bond length	r_s (in Å)	r_o (in Å)	r_{dft} (in Å)
$r(C_1-C_2)$		1.432(2)	1.429
$r(C_2-C_3)$	1.421(1)	1.432(2)	1.428
$r(C_3-C_4)$	1.410(1)	1.432(2)	1.427
$r(C_4-C_5)$	1.423(1)	1.432(2)	1.427
$r(C_6-C_7)$		1.432(2)	1.428
$r(C_7-C_8)$	1.424(3)	1.432(2)	1.429
$r(C_8-C_9)$	1.421(3)	1.432(2)	1.426
$r(C_9-C_{10})$	1.440(3)	1.432(2)	1.428
$r(C_1-H_{et})$		3.692(2)	3.703
r(Fe−C_1)		2.049(5)	2.049
r(Fe−C_2)	2.035(7)	2.049(5)	2.046
r(Fe−C_3)	2.052(5)	2.049(5)	2.047
r(Fe−C_4)	2.052(5)	2.049(5)	2.052
r(Fe−C_5)	2.035(7)	2.049(5)	2.047
r(Fe−C_6)		2.049(5)	2.048
r(Fe−C_7)	2.049(5)	2.049(5)	2.049
r(Fe−C_8)	2.056(9)	2.049(5)	2.048
r(Fe−C_9)	2.056(9)	2.049(5)	2.050
r(Fe−C_{10})	2.049(5)	2.049(5)	2.052
$r(C_1-C_{1'})$		1.4214[b]	1.421
$r(C_{1'}-C_{2'})$		1.2173[b]	1.217

bond angle	$\angle_s$ (in deg)	$\angle_o$ (in deg)	$\angle_{dft}$ (in deg)
$C_7-C_6-C_{10}$	108.3(9)	108[b]	108
$C_2-C_1-C_{1'}$		126[b]	126
$C_5-C_1-C_{1'}$		126[b]	126
$C_{1'}-C_{2'}-H_{et}$		180[b]	180
−C≡CH_{et} "tilt angle"		2.75(6)	

[a] The approximate r_o structure is obtained from the least-squares fitting. The r_s structure is obtained using a Kraitchman analysis. The r_{dft} structure is the output of the theoretical calculation [B3PW91/Hay-Wadt (n+1) ECP] and, because vibrational corrections were not included, is an r_e structure. The listed error limits on the parameters are 1σ. [b] Obtained from the DFT calculation and used to calculate $r(C_{2'}-H_{et})$. See text for further details.

(46) Little, W. F.; Reilley, C. N.; Johnson, J. D.; Lynn, K. N.; Sanders, A. P. *J. Am. Chem. Soc.* **1964**, *86*, 1376−1381.
(47) Britton, W. E.; Kashyap, R.; El-Hashash, M.; El-Kady, M.; Herberhold, M.; *Organometallics* **1986**, *5*, 1029−1031.

Table 8. r_s Coordinates (in Å) Obtained from Kraitchman Analyses in the Principal Axis System of the Parent Molecule, ETHFE ($^{12}C_{12}{}^{1}H_{10}{}^{56}Fe$)

atom	$\|a_s\|$	$\|b_s\|$	$\|c_s\|$
^{54}Fe	0.381	0.178	0.020
^{57}Fe	0.379	0.178	0.036
H_{et}	3.979	2.573	0.044
$^{13}C_2$	1.107	0.943	1.162
$^{13}C_3$	0.261	1.994	0.715
$^{13}C_7$	1.400	1.169	1.156
$^{13}C_8$	2.284	0.139	0.717

Discussion

Gas phase structural parameters for ETHFE have been determined from microwave spectroscopic measurements. The structural parameters determined by using three different methods, least-squares fitting and Kraitchman analysis of the measured transitions and DFT calculations, agree within the uncertainties. Using the least-squares fit, with some parameters fixed, we find the bond distances between the Fe atom and the C atoms of the two Cp rings are 2.049(5) Å and the C−C bond distances of the Cp rings are 1.432(2) Å. The uncertainties in the parentheses are much larger than the statistical error contributions to the fit, because C_5 symmetry was assumed and these parameters are correlated with other parameters, which are not fit directly.

A comparison between the values of the $C_{2'}-H_{et}$ bond from the crystal structure[17] determined by X-ray diffraction and the gas phase structure by microwave spectroscopy shows the bond length is quite different. The value of the $C_{2'}-H_{et}$ bond length from X-ray diffraction is 0.773 Å, and the value obtained from the present least-squares analysis is 1.053(4) Å. This deviation is not a surprising result because the hydrogen atom positions are usually poorly determined using X-ray diffraction. We used the least-squares fit value for $r(C_1-H_{et})$ and subtracted the fixed values $[r(C_1-C_{1'}) + r(C_{1'}-C_{2'})]$, as discussed above, to get a value for $r(C_1-H_{et}) = 1.053$ Å. The value is in good agreement with the bond length in free acetylene[48] $r(C-H) = 1.058$ Å.

The average distance for Fe−C of the Cp ring from X-ray diffraction is 2.0 Å. This distance is significantly shorter than the value obtained from the least-squares fit, which is 2.049(5) Å. The distance from Fe to the H_{et} atom determined from the X-ray diffraction structure is 4.9 Å. This distance is also significantly shorter when compared with the value determined from Kraitchman analysis, 5.09(8) Å. The value of the *A*-rotational constant obtained using the X-ray structure is 1391 MHz, which is higher by 84 MHz when compared to results from the gas phase microwave experiment (see Table 5). The experimental and DFT calculated structures obtained for the molecule ETHFE show that the Cp rings are in an eclipsed conformation unlike ferrocene, which is staggered in the crystal[49] and eclipsed in the gas phase.[45] Any attempt to do a least-squares fit using a staggered conformation as a starting point did not converge, and this is consistent with the prediction from the theoretical calculations that the staggered conformation has a much higher energy when compared to the eclipsed conformer. A single point energy calculation predicts the difference in energy between the eclipsed and staggered conformers to be 3 kJ/mol, with the eclipsed conformer being more stable. This calculation was done using the rB3PW91 method and using the Hay and Wadt (n+1) basis set with an effective core potential for iron and the split-valence plus polarization basis set (SVP) for the carbon and hydrogen atoms.

The "tilt angle" is defined to be the angle that the substituent (in our case, the −C≡C−H group) makes with the carbon plane of the substituted Cp ring. From previous studies in this lab, this angle was consistently shown to have a nonzero value. In the case of chloroferrocene,[18] the value of the "tilt angle" is 2.7(6)°, and for dimethylferrocene,[20] the value for this angle is 2.66(2)°. For the case of this molecule, the "tilt angle" determined from the least-squares fit is 2.75(6)°, in the direction away from the Fe atom. All of the theoretical methods and basis sets described in the theoretical section of this paper predict this "tilt angle" to be 0.1°. A DFT calculation fixing the "tilt angle" at the experimental value while optimizing the other parameters predicted the energy to be 0.02 kcal/mol higher when compared to the value obtained when all of the structural parameters were optimized. Calculations where the tilt angle was varied indicated a nearly flat variation of the energy with the tilt angle, for small values of this angle. These calculations were done using the rB3PW91 method and the Hay and Wadt (n+1) basis set with an effective core potential for iron and the split-valence plus polarization basis set (SVP) for the carbon and hydrogen atoms. The X-ray diffraction study indicates the "tilt angle" to be 1.7°, which is close to the present experimental value. Similar values for the "tilt angle" are obtained from both the X-ray and the microwave measurements, and we believe that they are probably due to the repulsion between π electrons of −C≡C−H and the valence electrons of the iron atom.

The linear correlation between the structural parameter r(Fe−Cp) and the Hammett parameter $\Sigma\sigma_I$ is shown in Figure 3. The reason for this linear correlation is due to the variation of the inductive effect of the substituent. This alters the electron density of the Cp ring. There is an increase in electron density as the electronegativity of the substituent group decreases. This affects the binding of the Fe−π−Cp ligand. This effect is normally reflected as a decrease in the binding energy and the ionization energy of the complex. Indeed, a study using electron spectroscopy for chemical analysis on methyl substitutions on the Cp ring has indicated that the binding energy between the metal atom and the Cp ring decreases with increasing methyl substitutions.[50] It is also seen that there is an increase in the ionization energies with the increasing electron-withdrawing nature of the substituent.[14] This effect is also observed in the measurement of the oxidation potential in nonaqueous solvents, with the oxidation potential shifting to a more positive direction as

(48) Harmony, M. D.; Laurie, V. W.; Kuczkowski, R. L.; Schwendeman, R. H.; Ramsay, D. A.; Lovas, F. J.; Lafferty, W. J.; Maki, A. G. *J. Phys. Chem. Ref. Data* **1979**, *8*, 619−721.
(49) Baun, W. L. *Anal. Chem.* **1959**, *31*, 1308−1311.
(50) Gassman, P. G.; Macomber, D. W.; Hershberger, J. W. *Organometallics* **1983**, *2*, 1470−1472.

Table 9. Structural Parameters of Different Ferrocene Compounds, $(C_5H_4-Y)-Fe-(C_5H_4-X)$, Relative Oxidation Potentials at Ambient Temperatures,[a] and Hammett Substituent Constants ($\Sigma\sigma_I$) for Cp Ligands[b,c]

name	X	Y	r(C−C)	r(Fe−Cp)	$\Delta E°$	$\Sigma\sigma_I$
chloroferrocene[d]	Cl	H	1.433(2)	1.610(5)	0.195	0.47
bromoferrocene[d]	Br	H	1.433(1)	1.630(2)	0.165	0.44
methylferrocene[d]	CH_3	H	1.4289(2)	1.6528(3)	−0.06	−0.04
dimethylferrocene[d]	CH_3	CH_3	1.434(5)	1.670(2)	−0.115	−0.08
ETHFE	C≡CH	H	1.432(2)	1.6464(1)	0.110	0.21
ferrocene[e]	H	H	1.440(2)	1.661(2)	0.0	0

[a] The values of $\Delta E°$ are obtained from refs 46 and 47. [b] The values of σ_I are obtained from ref 12. [c] The distances are given in units of Å, and the error limits (1σ) are given within the parentheses. The values of the oxidation potentials are given in volts. [d] The values are obtained from refs 18,19,20, and 21. [e] The values are obtained from electron diffraction data, ref 45.

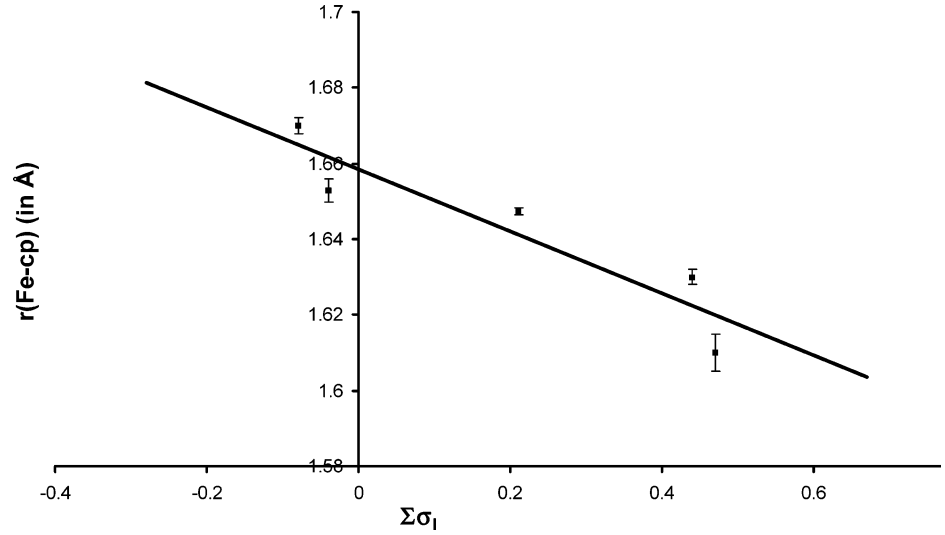

Figure 3. Plot showing the result of a linear regression analysis correlating the r(Fe−Cp) distance and $\Sigma\sigma_I$ of the substituent. The units of the distances are Å. This plot is governed by the equation $r(\text{Fe}-\text{Cp}) = -0.0821\Sigma\sigma_I + 1.6585$, with a value of $r = 0.93$.

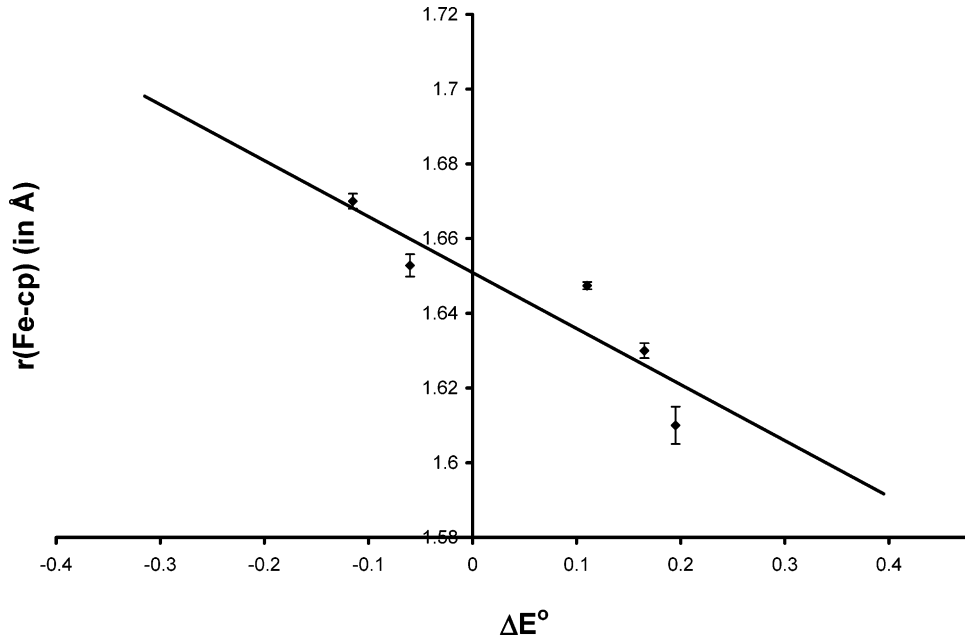

Figure 4. Plot showing the result of a linear regression analysis between the r(Fe−Cp) distance and $\Delta E°$ of the substituent. The units of the distances are Å, and $\Delta E°$ is in V. This plot is governed by the equation $r(\text{Fe}-\text{Cp}) = -0.1499\Delta E° + 1.6509$, with a value of $r = 0.91$.

the electron-withdrawing nature of the substituent increases.[46,47] This effect is seen in gas phase Fourier transform microwave spectroscopy as a decrease in the r(Fe−Cp) distance as the electronegativity of the substituent increases and is displayed by the plots shown in Figures 3 and 4.

From eqs 1 and 2, which accurately describe the data plotted in Figures 3 and 4, one can deduce the gas phase r(Fe−Cp) distance of ferrocene. The value of $\Sigma\sigma_I$ in the case of ferrocene is zero, and this gives a value of r(Fe−Cp) from eq 1 of 1.66 Å. Using eq 2 and knowing that the oxidation

potential ($\Delta E°$) for ferrocene is 0.0 V, one obtains the r(Fe−Cp) value 1.65 Å. It can be seen that the two independent methods of analysis reproduce the r(Fe−Cp) distance for ferrocene within 1%. This value of r(Fe−Cp) for ferrocene of 1.65(1) Å, determined as described, falls within 1% of the electron diffraction value[45] of 1.66 Å.

In conclusion, the near complete gas phase structure of ETHFE has been obtained. The present data set with multiple isotopomers allows us to determine, with high accuracy and precision, the positions of the various heavy atoms in the structure. The present work also indicates that the compound exists in the gas phase as an eclipsed conformer, with a slight tilt of the ethynyl group away from the Fe atom. The present work, in combination with the previous work on substituted ferrocene compounds, presents a coherent picture of the effect of substitution on the Cp rings. From this picture, we have been able to deduce the distance from the Fe atom to the center of the Cp ring for a molecule with no dipole moment, namely, ferrocene, using microwave spectroscopy.

Acknowledgment. This paper is based upon work supported by the National Science Foundation under Grant CHE-0304969. This support from the National Science Foundation is gratefully acknowledged. We thank Prof. Robin Polt, University of Arizona, for useful suggestions during the synthesis of the deuterated ethynylferrocene.

IC048516X